View Online / Journal Homepage / Table of Contents for this issue
Dynamic Article Links

Journal of Materials Chemistry

Cite this: J. Mater. Chem., 2012, 22, 4603

www.rsc.org/materials

COMMUNICATION

Optically tunable arrayed structures for highly sensitive plasmonic detection *via* simplified holographic lithography†

Hwan Chul Jeon, Chul-Joon Heo, Su Yeon Lee, Sung-Gyu Park and Seung-Man Yang*

Received 8th November 2011, Accepted 9th January 2012
DOI: 10.1039/c2jm15723c

Published on 23 January 2012 on http://pubs.rsc.org | doi:10.1039/C2JM15723C
Downloaded by Chengdu Library of Chinese Academy of Science on 07 March 2012

Hexagonally arranged plasmonic dot arrays were fabricated using simplified holographic lithography, electron-beam evaporation and lift-off processes. In our strategy, we used face-centered cubic structures as metal deposition masks which were created by prism holographic lithography. The features of plasmonic dot arrays such as arrangements, shapes, and sizes depended on the number of face-centered cubic structure layers and the laser exposure dose. The arrays showed tunable optical properties and were useful for surface-enhanced Raman scattering.

In recent years, periodic metallic nanostructure arrays with tunable optical properties have been widely studied for their potential use in a variety of fascinating applications. Localized surface plasmon resonance (LSPR), observed in metal nanoparticle arrays interacting with an incident light field,[1] is an emerging research area for biochemical sensors and precisely designed nanoantennas.[2–4] The properties of an LSPR depend strongly on nanostructure geometry and small changes in the local environment; hence the plasmonic properties can be easily tuned by varying the type, size, shape and arrangement of metal nanoparticles and the local array environment.[2–4] Various techniques have been developed to fabricate tunable plasmonic structures, such as electron-beam lithography[2,4] or nanosphere lithography.[3] However, electron-beam lithography is a time-consuming technique because of the demanding precisions and serial nature of the fabrication procedure; in the case of nanosphere lithography it is difficult to fabricate nanostructures over large areas without defects.

Holographic lithography (HL) provides a facile route to fabricating 1D, 2D, and 3D periodic structures using optical interference among two or more beams.[5] This strategy can be used to rapidly fabricate defect-free submicrometre-scale structures over a large area. Recently, specially designed prisms have been introduced to create multiple beams from a single laser beam through refraction[6] or total internal reflection[7] to overcome the disadvantages of the multi-beam HL, which are the complexities of aligning an optical setup and controlling the optical path lengths. These HL-derived inter-connected nanostructures have been used for various applications, including photonic applications,[5–7] microfluidic sensing and mixing applications,[8] and micro- or nanoporous templates for infiltration of polymer, metal, or self-assembled colloidal nanoparticles.[9]

Here, we demonstrate a unique method for fabricating uniformly ordered plasmonic arrays over a large area using prism HL-featured face-centered cubic (FCC) structures as masks for directional metal deposition. The arrangements, geometrical features, and optical properties of the metallic nanostructures resulting from the lift-off process strongly depended on the fabrication conditions of the polymeric masks: (1) the number of FCC hexagonal layers, which is determined by the thickness of the photoresist (PR) and (2) the laser exposure time during the prism HL process. A variety of metallic dot arrays with tunable plasmonic resonances in the near-infrared (NIR) region were fabricated; moreover, unique 3-split ring arrays composed of 3 elliptical dots demonstrated potential for highly sensitive molecular detection based on strong local electromagnetic (EM) field enhancement in the interparticle region.

Scheme 1 shows the fabrication procedure, consisting of five steps. An SU-8 PR was spin-coated onto the glass wafer with a pre-coated Omni-coat as a sacrificial layer. The thickness of the PR could be controlled by the epoxy-based PR resin concentration and the spin speed. The polymeric FCC structures were fabricated using HL with a single top-cut prism, which generated four beams from a single beam (see Fig. S1, ESI†). The number of FCC structure layers could be varied according to the PR thickness. SF_6 reactive ion etching (RIE) was performed to remove the sacrificial layer from the vacant spaces. After deposition of a 60 nm thick gold (Au) film using electron-beam evaporation, the polymeric masks could be released from the glass substrate by dissolving the pre-coated sacrificial layer using a developer under ultra-sonication.

Fig. 1 shows scanning electron microscopy (SEM) images of the polymeric FCC structures after RIE and the resulting plasmonic Au dot large-area arrays after the deposition and lift-off processes for the 1-layered and 2-layered cases. The electron micrograph in Fig. 1a shows a hexagonal array of circular holes with a 705 nm periodicity and a hole diameter of 450 nm. A hexagonal array of three elliptical holes with 710 nm periodicity is shown in Fig. 1b. The minor axis (*a*) of each hole was 161 nm and the major axis (*b*) was 320 nm. SEM images permitted measurement of the heights of the PR layers: 210 nm for the 1-layered and 960 nm for 2-layered FCC structures, respectively (see Fig. S2, ESI†). The resulting FCC structures, which

National CRI Center for Integrated Optofluidic Systems, Department of Chemical and Biomolecular Engineering, KAIST, Daejeon, 305-701, Korea. E-mail: smyang@kaist.ac.kr; Fax: +82 42-350-5962

† Electronic supplementary information (ESI) available: Schematics of setup for prism holographic lithography, beam arrangement, and SEM images. See DOI: 10.1039/c2jm15723c

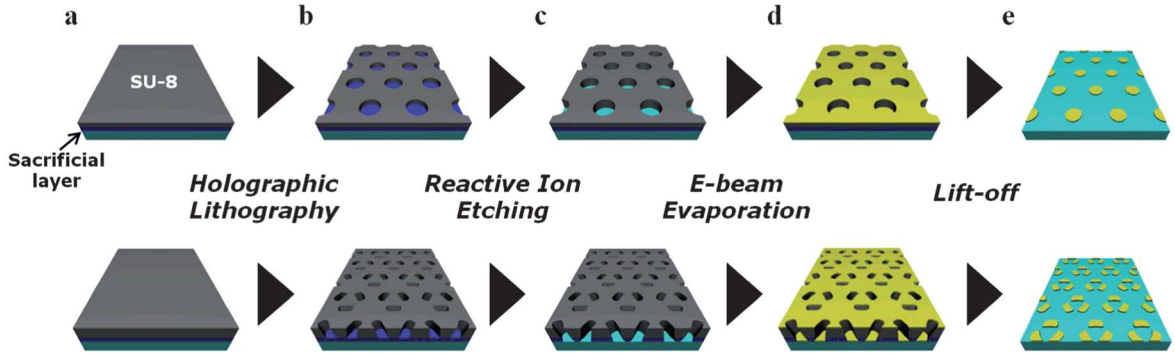

Scheme 1 Schematic diagram illustrating the fabrication of uniformly ordered tunable plasmonic arrays using HL-derived FCC structures as deposition masks, produced by the 1-layered (first row) and 2-layered (second row) cases. (a) Spin-coating of the SU-8 PR on a substrate with a pre-coated sacrificial layer. (b) SU-8 structures resulting from HL using a single top-cut prism. (c) RIE to remove the sacrificial layer. (d) Deposition of the Au thin film *via* electron-beam evaporation. (e) Plasmonic nanodot arrays resulting from the lift-off process.

Downloaded by Chengdu Library of Chinese Academy of Science on 07 March 2012
Published on 23 January 2012 on http://pubs.rsc.org | doi:10.1039/C2JM15723C

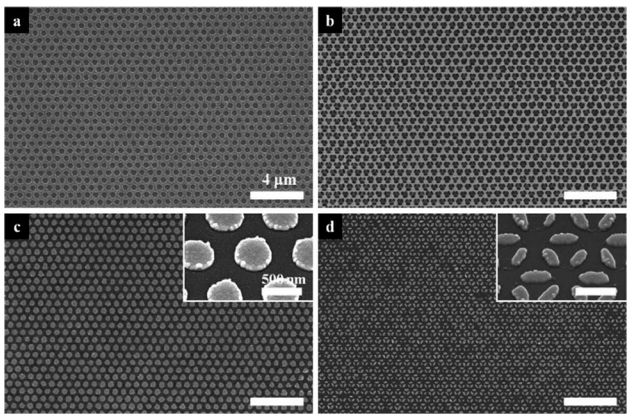

Fig. 1 Large area SEM images of the fabricated (a) 1-layered and (b) 2-layered polymeric FCC structures used as masks and plasmonic arrays prepared from (c) 1-layered and (d) 2-layered masks, respectively. The insets of (c) and (d) show magnified 40° tilted views of the SEM images of Au nanostructures.

were used as deposition masks for Au deposition, have quite a large uniform area of an equilateral triangle with 0.4 cm side length within a second of laser exposure.[8] The Au deposition and mask removal steps produced Au nanodot arrays with different shapes and arrangements, determined by the geometries of the patterned masks (Fig. 1c and d). The average diameter of the circular Au dots was 454 nm and the periodicity was 705 nm (Fig. 1c). As shown in Fig. 1d, a 3-split ring array composed of elliptical dots ($a = 165$ nm, $b = 323$ nm) was prepared with 710 nm periodicity over a large area (see Fig. S3, ESI†).

The main advantage of using HL for plasmonic array fabrication is that geometric features can be easily controlled by varying the laser exposure dose, compared to other techniques such as electron-beam lithography and nanosphere lithography.[8] In this manner, the hole size of the FCC structures, which determines the size of the resulting Au dots, could be tuned. Fig. 2 shows the FCC structure mask hole size as a function of laser exposure dose. The diameters of the holes were measured from the SEM images. As the laser exposure time increased from 0.4 s to 0.6 s in 0.1 s increments, the diameters of the circular holes decreased from 491 nm to 450 nm, and 403 nm for 1-layered FCC masks (Fig. 2a–c). The elliptical holes in the 2-layered FCC structure also became smaller from $a = 174$ nm, $b = 369$ nm to $a = 161$ nm, $b = 320$, and $a = 136$ nm, $b = 294$ nm at 0.21 s, 0.23 s, and 0.25 s of laser exposure, respectively (Fig. 2d–f).

The tunable holes of the polymeric FCC structures in Fig. 2 were used for directional Au deposition. The deposition and lift-off processes yielded various Au dot patterns on the substrate, depending on the shapes and sizes of the polymeric masks. Fig. 3 shows SEM images of two types of plasmonic dot arrays fabricated from the circular or elliptical hole arrays for the 1-layered (Fig. 3a–c) or 2-layered masks (Fig. 3d–f), respectively. The hexagonally ordered circular dot arrays of diameter 486 nm, 454 nm, and 415 nm were obtained by using the structures shown in Fig. 2a–c as deposition masks (Fig. 3a–c). The 2-layered FCC structure masks (Fig. 2d–f) yielded hexagonal arrays consisting of 3 elliptical dots, which resembled 3-split ring arrays,[4] with $a = 180$ nm, $b = 362$ nm (Fig. 3d), $a = 165$ nm, $b = 323$ (Fig. 3e), and $a = 141$ nm, $b = 304$ nm (Fig. 3f). The feature dimensions of the masks and the resulting dots were well matched.

Plasmonic dot arrays formed under longer exposure times were prepared to determine the tunability limits. The exposure conditions were 0.7 s and 0.27 s for the 1-layered and 2-layered masks, respectively (see Fig. S4, ESI†). Further increases in the laser exposure time yielded Au deposition holes that were too small to permit Au thin film deposition through the holes. Even if the Au was deposited

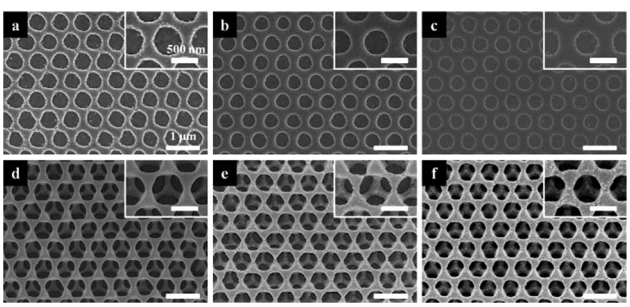

Fig. 2 SEM images of polymeric masks after RIE with various laser exposure times for 1-layered structures with (a) 0.4 s, (b) 0.5 s and (c) 0.6 s, and for 2-layered structures with (d) 0.21 s, (e) 0.23 s and (f) 0.25 s, respectively. The insets of (a)–(f) show magnified views of the SEM images.

 This journal is © The Royal Society of Chemistry 2012

Downloaded by Chengdu Library of Chinese Academy of Science on 07 March 2012
Published on 23 January 2012 on http://pubs.rsc.org | doi:10.1039/C2JM15723C

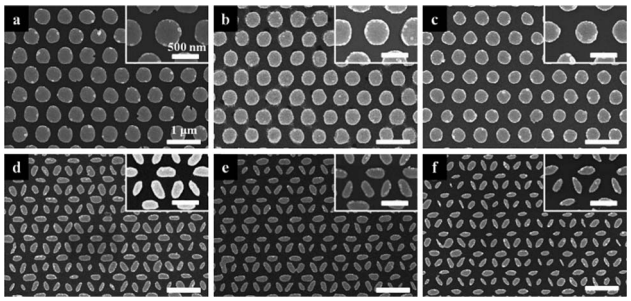

Fig. 3 SEM images of the tunable plasmonic arrays after the lift-off process developed from 1-layered masks with (a) 0.4 s, (b) 0.5 s and (c) 0.6 s, and 2-layered masks with (d) 0.21 s, (e) 0.23 s and (f) 0.25 s of laser exposure times, respectively. The insets of (a)–(f) show magnified views of the SEM images.

through the masks, the resulting small Au nanostructures detached irregularly from the glass substrate during the lift-off process with ultra-sonication due to weak adhesion to the substrate.

Although we thought it might be possible to fabricate a hexagonal array consisting of 6 triangular dots using a 3-layered FCC structure deposition mask, unfortunately, this was experimentally difficult to achieve due to size limitations on directional metal deposition (see Fig. S5, ESI†).

The optical properties of the Au nanodot arrays were investigated using a home-built visible-to-near-infrared spectroscopy.‡[3] The absorbance spectra of the nanostructures shown in Fig. 3 were recorded under white light illumination with normal incidence (Fig. 4). Absorbance peaks were observed in the NIR region, indicating the presence of a resonance due to the hexagonally arranged Au dot arrays. The absorbance peak was blue-shifted at higher exposure doses, which reduced the diameter of the segments without affecting the periodicity (705 nm) for the 1-layered mask (Fig. 4a). The circular Au dot arrays 486 nm in diameter (0.4 s) exhibited an extinction at 1270 nm. Plasmonic arrays 454 nm (0.5 s) or 415 nm in diameter (0.6 s) showed resonances at 1170 nm or 1080 nm, respectively. The same tendency was observed for the 2-layered cases (Fig. 4b). The absorbance peaks were blue-shifted (from 1192 nm to 1064 nm, and 968 nm) at longer laser exposure times (from 0.21 s to 0.23 s, and 0.25 s). The lengths of the major and minor axes of the elliptical segments changed with the exposure time without affecting the periodicity (710 nm) or elliptical ratio (b/a, 2.0). The structural features of the nanostructures, including the size, shape, and arrangement, were responsible for certain spectral positions of the plasmonic resonance.[1–4] The peak intensities at higher exposure doses decreased due to reduced nanostructure coverage over the substrate. We suggested that differences in the optical properties based on geometric effects could be applied to plasmonic sensing applications.[3,4]

The utility of the prepared plasmonic structures as sensors was tested in the context of surface-enhanced Raman scattering (SERS). Target molecules were adsorbed onto the surfaces of the Au nanostructures by immersing the samples in ethanolic solutions of 2 mM benzenethiol (BT) for 8 h. After washing with ethanol several times, Raman spectra were collected over 10 s using a high-resolution dispersive Raman microscope.‡ Fig. 5 shows the SERS spectra of BT adsorbed onto four different plasmonic substrates, and the spectrum was compared with that from a smooth flat Au film as a reference. The characteristic peaks of BT, at 994, 1017, 1071, and 1571 cm^{-1}, were not observed for the smooth Au thin film. Interparticle coupling can enhance the magnitude of an EM field due to the plasmonic resonance;[1–4] hence variations in the separation distance (d) among adjacent particles can strongly affect the local EM field enhancement.[10] It was difficult to achieve strong Raman signals from the Au dot arrays prepared from 1-layered masks. A representative spectrum (0.4 s exposure and d = 221 nm) is plotted in cyan in Fig. 5. The samples developed from 2-layered masks yielded SERS peak intensities that were much stronger due to coupling effects originating from closely spaced structures. Strong enhancements were observed from the nanostructures with small interparticle distances (d = 90 nm,

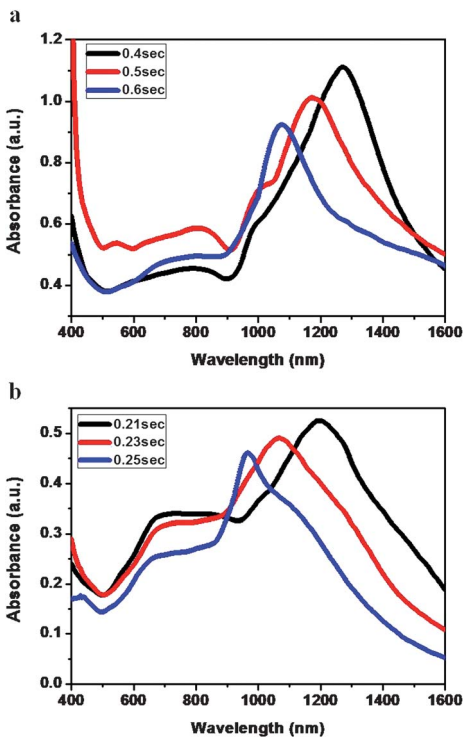

Fig. 4 Measured absorbance spectra obtained from hexagonally ordered tunable plasmonic nanodot arrays for the (a) 1-layered and (b) 2-layered cases, as a function of the laser exposure time.

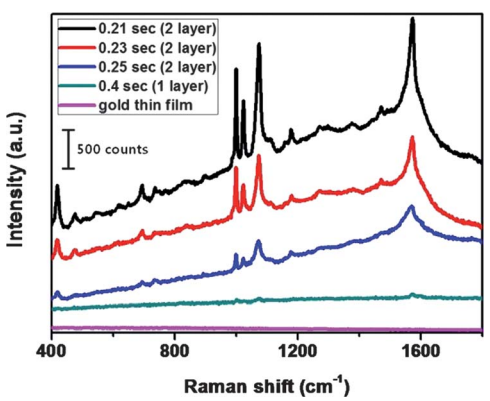

Fig. 5 SERS spectra of BT-adsorbed tunable plasmonic nanodot arrays under various experimental conditions. Data acquisition involved a 10 s accumulation, repeated ten times, and the laser power was 1.7 mW.

0.21 s exposure), in contrast with the structures having $d = 110$ and 146 nm (developed from 0.23 s and 0.25 s exposures, respectively). The plasmonic structures prepared by HL may potentially be used as microfluidic sensor devices by integrating the structures into microfluidic chips in combination with conventional photolithographic techniques.[8]

In conclusion, we report a novel method for fabricating tunable plasmonic dot arrays over a large area using HL to produce 1- and 2-layered FCC structures as masks for metal deposition. The arrangements, shapes, and sizes of the resulting dot arrays could be precisely controlled by changing the thickness of the PR and the laser exposure dose during prism HL. A variety of Au dot arrays with different plasmonic resonances in the NIR were fabricated by controlling the laser exposure time. Furthermore, 3-split ring arrays composed of 3 elliptical dots demonstrated utility for highly sensitive molecular recognition based on strong local EM field enhancement in the interparticle region. Such plasmonic structures were expected to be useful for a wide range of applications, especially in chemical and biomolecular sensing micro-devices based on LSPR.

Acknowledgements

This work was supported by a grant from the Creative Research Initiative Program of the Ministry of Education, Science and Technology for "Complementary Hybridization of Optical and Fluidic Devices for Integrated Optofluidic Systems." Partial support from the Brain Korea 21 Program is also appreciated.

Notes and references

‡ *Characterization*: The morphologies of the surface and cross-section of the samples were investigated by field emission-scanning electron microscopy (Hitachi S-4800). The optical properties of the resulting plasmonic arrays were analyzed using a home-built visible-to-near-infrared spectroscopy setup over the range 400–1600 nm with a beam diameter of 100 μm. The Raman spectra were measured using a high-resolution dispersive Raman microscope (Horiba Jobin Yvon, LabRAM HR UV/Vis/NIR), in which a 633 nm laser with a power of 1.7 mW was focused on the sample surface with a beam diameter of 1 μm.

1 W. A. Murray and W. L. Barnes, *Adv. Mater.*, 2007, **19**, 3771.
2 M. Hentschel, M. Saliba, R. Vogelgesang, H. Giessen, A. P. Alivisatos and N. Liu, *Nano Lett.*, 2010, **10**, 2721.
3 C. J. Heo, S. H. Kim, S. G. Jang, S. Y. Lee and S. M. Yang, *Adv. Mater.*, 2009, **21**, 1726.
4 A. W. Clark and J. M. Cooper, *Adv. Mater.*, 2010, **22**, 4025; A. W. Clark and J. M. Cooper, *Small*, 2011, **7**, 119.
5 M. Campbell, D. N. Sharp, M. T. Harrison, R. G. Denning and A. J. Turberfield, *Nature*, 2000, **404**, 53; J. H. Jang, C. K. Ullal, M. Maldovan, T. Gorishnyy, S. Kooi, C. Y. Koh and E. L. Thomas, *Adv. Funct. Mater.*, 2007, **17**, 3027; J. H. Moon, J. Ford and S. Yang, *Polym. Adv. Technol.*, 2006, **17**, 83.
6 L. J. Wu, Y. C. Zhong, C. T. Chan, K. S. Wong and G. P. Wang, *Appl. Phys. Lett.*, 2005, **86**, 241102.
7 Y. K. Pang, J. C. W. Lee, C. T. Ho and W. Y. Tam, *Opt. Express*, 2006, **14**, 9113.
8 S. K. Lee, S. G. Park, J. H. Moon and S. M. Yang, *Lab Chip*, 2008, **8**, 388; S. G. Park, S. K. Lee, J. H. Moon and S. M. Yang, *Lab Chip*, 2009, **9**, 3144.
9 Y. Xu, X. Zhu, Y. Dan, J. H. Moon, V. W. Chen, A. T. Johnson, J. W. Perry and S. Yang, *Chem. Mater.*, 2008, **20**, 1816; S. G. Park, M. Miyake, S. M. Yang and P. V. Braun, *Adv. Mater.*, 2011, **23**, 2749; M. Miyake, Y. C. Chen, P. V. Braun and P. Wiltzius, *Adv. Mater.*, 2009, **21**, 3012; D. Y. Xia and S. R. J. Brueck, *Nano Lett.*, 2004, **4**, 1295.
10 Y. Yokota, K. Ueno and H. Misawa, *Small*, 2011, **7**, 252; S. K. Yang, W. P. Cai, L. C. Kong and Y. Lei, *Adv. Funct. Mater.*, 2010, **20**, 2527; N. A. Hatab, C. H. Hsueh, A. L. Gaddis, S. T. Retterer, J. H. Li, G. Eres, Z. Y. Zhang and B. H. Gu, *Nano Lett.*, 2010, **10**, 4952; M. E. Abdelsalam, S. Mahajan, P. N. Bartlett, J. J. Baumberg and A. E. Russell, *J. Am. Chem. Soc.*, 2007, **129**, 7399; L. Gunnarsson, E. J. Bjerneld, H. Xu, S. Petronis, B. Kasemo and M. Kall, *Appl. Phys. Lett.*, 2001, **78**, 802.

Downloaded by Chengdu Library of Chinese Academy of Science on 07 March 2012
Published on 23 January 2012 on http://pubs.rsc.org | doi:10.1039/C2JM15723C

 This journal is © The Royal Society of Chemistry 2012